

## Highly Frequent Frameshift DNA Synthesis by Human DNA Polymerase $\mu$

YANBIN ZHANG, XIAOHUA WU, FENGHUA YUAN, ZHONGWEN XIE, AND ZHIGANG WANG\*

*Graduate Center for Toxicology, University of Kentucky, Lexington, Kentucky 40536*

Received 11 April 2001/Returned for modification 24 May 2001/Accepted 28 August 2001

**DNA polymerase  $\mu$  (Pol $\mu$ ) is a newly identified member of the polymerase X family. The biological function of Pol $\mu$  is not known, although it has been speculated that human Pol $\mu$  may be a somatic hypermutation polymerase. To help understand the *in vivo* function of human Pol $\mu$ , we have performed *in vitro* biochemical analyses of the purified polymerase. Unlike any other DNA polymerases studied thus far, human Pol $\mu$  catalyzed frameshift DNA synthesis with an unprecedentedly high frequency. In the sequence contexts examined,  $-1$  deletion occurred as the predominant DNA synthesis mechanism opposite the single-nucleotide repeat sequences AA, GG, TT, and CC in the template. Thus, the fidelity of DNA synthesis by human Pol $\mu$  was largely dictated by the sequence context. Human Pol $\mu$  was able to efficiently extend mismatched bases mainly by a frameshift synthesis mechanism. With the primer ends, containing up to four mismatches, examined, human Pol $\mu$  effectively realigned the primer to achieve annealing with a microhomology region in the template several nucleotides downstream. As a result, human Pol $\mu$  promoted microhomology search and microhomology pairing between the primer and the template strands of DNA. These results show that human Pol $\mu$  is much more prone to cause frameshift mutations than base substitutions. The biochemical properties of human Pol $\mu$  suggest a function in nonhomologous end joining and V(D)J recombination through its microhomology searching and pairing activities but do not support a function in somatic hypermutation.**

Many cellular processes require a DNA polymerase (Pol), including DNA replication, DNA repair, recombination, translesion DNA synthesis, and somatic hypermutation. Pol $\alpha$ , Pol $\delta$ , Pol $\epsilon$ , and Pol $\gamma$  are replicative DNA polymerases in eukaryotes (16, 29). Pol $\zeta$  is a major polymerase required for DNA damage-induced mutagenesis (21, 22). Pol $\theta$  is likely involved in repair of DNA interstrand cross-links (27). Pol $\eta$ , Pol $\iota$ , and Pol $\kappa$  belong to the Y (UmuC) family of DNA polymerases and are involved in error-free and error-prone translesion synthesis opposite various DNA lesions (9, 20, 24, 31).

Pol $\beta$  is a major repair synthesis polymerase during base excision repair in higher eukaryotes (17, 33, 36). Pol $\beta$  and terminal deoxynucleotidyltransferase (TdT) are members of the DNA polymerase X family (13). TdT catalyzes nucleotide addition to DNA in a template-independent manner (3, 5). This enzyme is restricted to lymphoid tissues and functions during V(D)J recombination of the immunoglobulin genes and T-cell receptor genes (3, 5, 32). Most recently, the two newest members of the DNA polymerase X family, designated Pol $\lambda$  and Pol $\mu$ , have been identified in humans (1, 8, 10). According to protein sequence comparisons, Pol $\lambda$  is more closely related to Pol $\beta$  while Pol $\mu$  is phylogenetically closer to TdT (1, 8). The biological functions of Pol $\lambda$  and Pol $\mu$  remain to be defined. It has been speculated that Pol $\lambda$  may play a role in meiosis (10) and that Pol $\mu$  may be a somatic hypermutation polymerase (8).

V(D)J recombination and somatic hypermutation are two essential mechanisms for generating antibody diversity during immunoglobulin development. V(D)J recombination requires DNA strand cleavage by the lymphoid-specific RAG1 and

RAG2 proteins, and the resulting double-strand breaks are repaired by a nonhomologous end joining (NHEJ) mechanism similar to that employed by other tissues to repair the broken ends of DNA. Proteins involved in NHEJ include Ku70, Ku80, DNA-PK $\epsilon$ , XRCC4, and DNA ligase IV (25). More proteins are likely needed during NHEJ, such as a specific factor that promotes microhomology search and microhomology pairing. Somatic hypermutation introduces mainly point mutations into the V region of immunoglobulin genes at a rate of  $10^{-3}$  to  $10^{-4}$ /base pair/generation, which is  $\approx 10^6$ -fold higher than the spontaneous mutation rate in the rest of the genome (30). Thus, somatic hypermutation probably requires a low-fidelity DNA polymerase that possesses extraordinarily high error rates of misincorporations opposite undamaged template bases (4). However, this hypothetical hypermutation polymerase has eluded extensive studies thus far.

To help understand the biological function of human Pol $\mu$ , we have extensively analyzed its biochemical properties. Surprisingly, we found that human Pol $\mu$  catalyzes frameshift DNA synthesis with an unprecedentedly high frequency. Furthermore, when the primer 3' end contains base mismatches, human Pol $\mu$  efficiently realigns the primer strand to form new base pairings further downstream with the template bases. These remarkable biochemical properties do not support a role for human Pol $\mu$  in somatic hypermutation and suggest that human Pol $\mu$  may function in NHEJ and V(D)J recombination by promoting microhomology search and microhomology pairing.

### MATERIALS AND METHODS

**Materials.** A mouse monoclonal antibody against the His $_6$  tag was purchased from Qiagen (Valencia, Calif.). Alkaline phosphatase-conjugated anti-mouse immunoglobulin G was from Sigma Chemical Co. (St. Louis, Mo.). Oligonucleotides were synthesized by Operon (Alameda, Calif.). The yeast *rad30* deletion

\* Corresponding author. Mailing address: 306 Health Sciences Research Bldg., Graduate Center for Toxicology, University of Kentucky, Lexington, KY 40536. Phone: (859) 323-5784. Fax: (859) 323-1059. E-mail: zwang@pop.uky.edu.

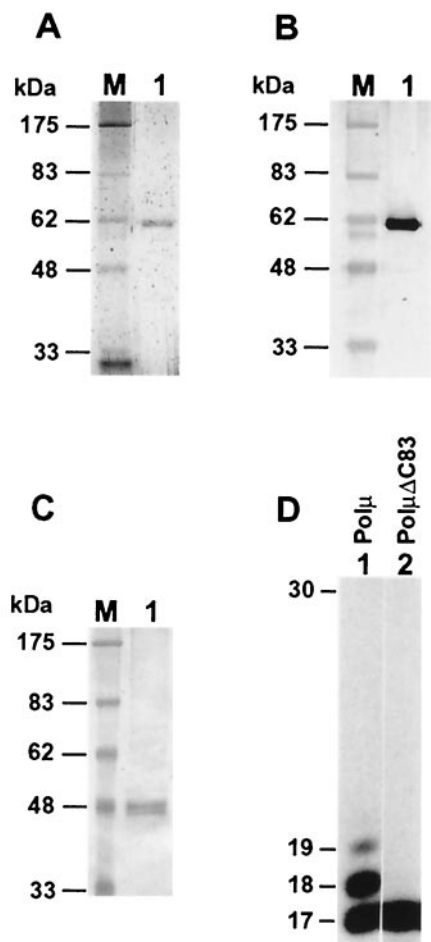


FIG. 1. Analysis of purified human Pol $\mu$ . (A) Purified human Pol $\mu$  (300 ng) was analyzed by electrophoresis on an SDS-10% polyacrylamide gel and visualized by silver staining. Protein mass markers (lane M) are indicated on the left. (B) Purified human Pol $\mu$  (300 ng) was analyzed by Western blotting using a mouse monoclonal antibody against the N-terminal His<sub>6</sub> tag. (C) The mutant human Pol $\mu$  (Pol $\mu$ ΔC83) was partially purified on a Ni column, and the sample (700 ng) was analyzed by Western blotting using the mouse monoclonal antibody against the N-terminal His<sub>6</sub> tag. (D) The Ni column fractions containing similar amounts of human Pol $\mu$  and Pol $\mu$ ΔC83 as determined by a Western blot analysis were assayed for DNA polymerase activity, using the template 5'-GGATGGACTGCAGGATCCGGAG GCCGCGC annealed with the 5' <sup>32</sup>P-labeled primer 5'-CGCGCG GCCTCCGGATC. The Pol $\mu$ ΔC83 sample contained 70 ng of total proteins in the polymerase assay. DNA size markers in nucleotides are indicated on the left.

mutant strain BY4741rad30Δ (*MATα his3 leu2 met15 ura3 rad30Δ*) was purchased from Research Genetics (Huntsville, Ala.). The Klenow fragment of *Escherichia coli* DNA polymerase I was purchased from Gibco BRL (Bethesda, Md.), *Pfu* DNA polymerase was obtained from Stratagene (La Jolla, Calif.), and restriction endonucleases were from New England Biolabs (Beverly, Mass.). Human Pol $\beta$  was purified to apparent homogeneity as previously described (38).

**Gene constructions.** Human Pol $\mu$  is encoded by the *POLM* gene (1, 8). The *POLM* cDNA was obtained by PCR amplification from human pancreas cDNAs using *Pfu* DNA polymerase and two primers, 5'-GCTCTAGAGTCGACATGC TCCCAAACGGCGG (PolMF primer) and 5'-ACATGCATGCAGGCCCA CCACAGC. The resulting 1.8-kb PCR product was then cloned into the *Sa*II and *Sph*I sites of the vector pEGU6, yielding pEGU6-POLM. The *POLM* gene was verified by DNA sequencing. This expression construct contains the 2 $\mu$ m origin for multicopy plasmid replication, the *URA3* gene for plasmid selection,

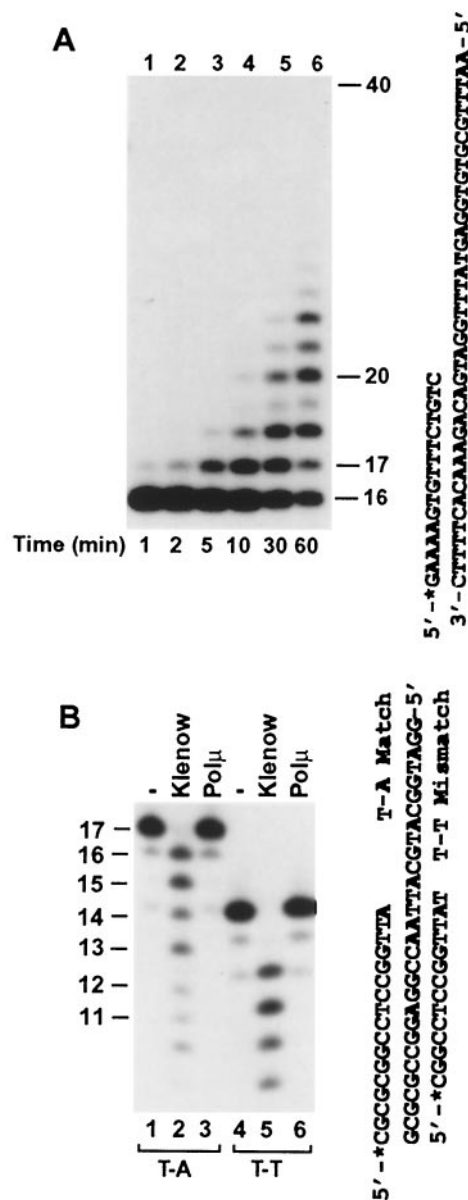


FIG. 2. Assays for distributive DNA synthesis and proofreading exonuclease of human Pol $\mu$ . (A) DNA polymerase assays were performed with 1.5 ng (27 fmol) of human Pol $\mu$  at 30°C for various times as indicated, using a 40-mer DNA template containing a 16-mer 5' <sup>32</sup>P-labeled (asterisk) primer as shown on the right. (B) DNA substrates (50 fmol) containing a T-A (template-primer) pair (lanes 1 to 3) or a T-T mismatch (lanes 4 to 6) (sequences shown on the right) at the primer 3' end were incubated with purified human Pol $\mu$  (5 ng; 90 fmol) for 10 min at 37°C in the DNA polymerase assay buffer without dNTPs. Similar assays were performed with the purified Klenow fragment (1 U) of *E. coli* DNA polymerase I, except that the incubation time was reduced to 2 min. The reaction products were separated by electrophoresis on a 20% denaturing polyacrylamide gel. Lanes 1 and 4, no DNA polymerase. DNA size markers in nucleotides are indicated on the sides.

the inducible *GAL1/GAL10* promoter, and six histidine codons preceding the ATG initiator codon of the human *POLM* gene. To construct the mutant *polm* gene, the pEGU6-POLM plasmid was amplified by PCR with the PolMF primer and the primer 5'-CCCAAGCTTAGGATGGGACAGGGCCTCG. The resulting 1.2-kb DNA fragment was then cloned into the *Sa*II and *Hind*III sites

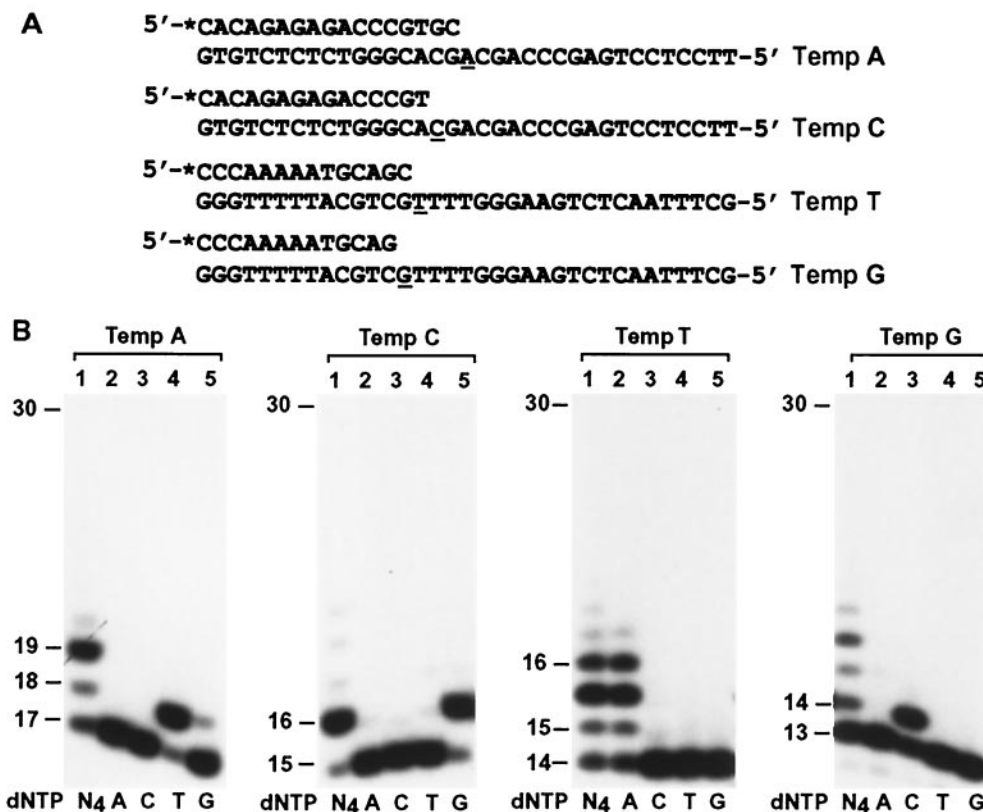


FIG. 3. Fidelity of human Pol $\mu$ . (A) Sequences from the JH4-JH5 intron of the rearranged human JH gene were used as DNA templates for polymerase assays; the analyzed template bases are underlined. Each primer was labeled at its 5' end with  $^{32}\text{P}$  as indicated by an asterisk. (B) Polymerase assays were performed with 50 fmol of DNA and 1.5 ng (27 fmol) of human Pol $\mu$  in the presence of a single dNTP (dATP [A], dCTP [C], dTTP [T], or dGTP [G]) or all four dNTPs (N<sub>4</sub>) as indicated. DNA size markers in nucleotides are indicated on the left.

of the vector pEGU6, yielding pEGU6-polm $\Delta$ C83. The mutant gene was verified by DNA sequencing. Expression of pEGU6-polm $\Delta$ C83 in yeast cells produces the mutant protein Pol $\mu$  $\Delta$ C83 missing the C-terminal 83 amino acids of human Pol $\mu$ .

**Purification of human Pol $\mu$ .** Yeast BY4741rad30 $\Delta$  cells harboring pEGU6-POLM were grown in minimum medium containing 2% sucrose for 2 days. Expression of Pol $\mu$  was induced by diluting the culture 10-fold in 16 liters of YPG (2% Bacto Peptone, 1% yeast extract, 2% galactose) medium supplemented with 0.5% sucrose and incubation for 15 h at 30°C with shaking. The collected cells ( $\approx$ 100 g) were homogenized with zirconium beads in a Bead-Beater (Biospec Products, Bartlesville, Okla.) in an extraction buffer containing 50 mM Tris-HCl, pH 7.5, 600 mM KCl, 5 mM  $\beta$ -mercaptoethanol, 10% sucrose, and protease inhibitors (37). The clarified extract ( $\approx$ 120 ml) was loaded onto two connected HiTrap chelating columns (5 ml each) charged with NiSO<sub>4</sub> (Amersham Pharmacia Biotech, Piscataway, N.J.), followed by washing the column sequentially with 100 ml of Ni buffer A (20 mM KH<sub>2</sub>PO<sub>4</sub>, pH 7.4, 0.5 M NaCl, 10% glycerol, 5 mM  $\beta$ -mercaptoethanol, and protease inhibitors) containing 10 mM imidazole and 100 ml of Ni buffer A containing 35 mM imidazole. Bound proteins were eluted with a linear gradient of 35 to 108 mM imidazole. The His<sub>6</sub>-tagged human Pol $\mu$  was identified by Western blot analyses using a mouse monoclonal antibody specific to the His<sub>6</sub> tag. The pooled sample ( $\approx$ 150 ml) was concentrated by polyethylene glycol 10,000 and desalted through 5 connected Sephadex G-25 columns (5 ml each) (Amersham Pharmacia Biotech) in fast-protein liquid chromatography (FPLC) buffer A (50 mM Tris-HCl, pH 7.5, 1 mM EDTA, 10% glycerol, and 5 mM  $\beta$ -mercaptoethanol) containing 80 mM KCl. The resulting sample ( $\approx$ 50 ml) was loaded onto an FPLC Mono S HR5/5 column (Amersham Pharmacia Biotech) and eluted with a 30-ml linear gradient of 80 to 600 mM KCl in FPLC buffer A. Human Pol $\mu$  was eluted at  $\approx$ 250 mM KCl. The Mono S fractions of human Pol $\mu$  were concentrated to 250  $\mu$ l by polyethylene glycol 10,000 and loaded onto an FPLC Superdex 200 gel filtration column that had been equilibrated in FPLC buffer A containing 150 mM KCl. Human Pol $\mu$  was eluted at the  $\approx$ 60-kDa position.

**DNA polymerase assays.** A standard DNA polymerase reaction mixture (10  $\mu$ l) contained 25 mM KH<sub>2</sub>PO<sub>4</sub> (pH 7.0), 5 mM MgCl<sub>2</sub>, 5 mM dithiothreitol, 100  $\mu$ g of bovine serum albumin/ml, 10% glycerol, 50  $\mu$ M deoxynucleoside triphosphates (dNTPs) (dATP, dCTP, dTTP, and dGTP individually or together as indicated), 50 fmol of a DNA substrate containing a  $^{32}\text{P}$ -labeled primer, and purified DNA polymerase as indicated. After incubation at 30°C for 10 min or as otherwise indicated, reactions were terminated with 7  $\mu$ l of a stop solution (20 mM EDTA, 95% formamide, 0.05% bromophenol blue, and 0.05% xylene cyanol). The reaction products were separated by electrophoresis on a 20% denaturing polyacrylamide gel and visualized by autoradiography.

**Kinetic analysis of human Pol $\mu$ .** Kinetic analysis of human Pol $\mu$  was performed as previously described (6, 38). Briefly, the assays were performed using 50 fmol of a DNA substrate containing a 5'  $^{32}\text{P}$ -labeled primer, 0.75 ng (14 fmol) of purified Pol $\mu$ , and increasing concentrations of each dNTP (dATP, dCTP, dTTP, or dGTP). Incubations were for 10 min at 30°C under standard DNA polymerase assay conditions. Longer incubations of up to 120 min were required to detect some misincorporations by human Pol $\mu$ . The reaction products were separated by electrophoresis on a 20% denaturing polyacrylamide gel and quantitated by scanning densitometry. The observed enzyme velocity ( $v$ ) was plotted as a function of dNTP concentration. The plotted data was fitted by a nonlinear regression curve to the Michaelis-Menton equation,  $v = (V_{\text{max}} \times [\text{dNTP}]) / (K_m + [\text{dNTP}])$ , using the SigmaPlot software.  $V_{\text{max}}$  and  $K_m$  values for the incorporation of the correct and the incorrect nucleotides were obtained from the fitted curves. The relative error rate ( $f_{\text{inc}}$ ) of nucleotide incorporation was calculated from the equation:  $f_{\text{inc}} = (V_{\text{max}}/K_m)_{\text{incorrect}} / (V_{\text{max}}/K_m)_{\text{correct}}$ .

## RESULTS

**Purification of human Pol $\mu$ .** Following its expression in yeast cells, we have purified human Pol $\mu$  to near homogeneity (Fig. 1A). The identity of human Pol $\mu$  was confirmed by West-

TABLE 1. Kinetic measurement of nucleotide incorporation by human Pol $\mu$ <sup>a</sup>

dNTP	$V_{\max}$ (fmol/min; mean $\pm$ SD)	$K_m$ ( $\mu$ M; mean $\pm$ SD)	$V_{\max}/K_m$	$f_{\text{inc}}^b$
Template A				
dATP	0.036 $\pm$ 0.0004	351.4 $\pm$ 183.3	0.00010	5.4 $\times$ 10 <sup>-5</sup>
dCTP	ND <sup>c</sup>	ND	0.00038	2.1 $\times$ 10 <sup>-4</sup>
dTTP	3.48 $\pm$ 0.17	1.89 $\pm$ 0.43	1.84	1
dGTP	2.13 $\pm$ 0.05	32.4 $\pm$ 2.55	0.066	3.6 $\times$ 10 <sup>-2</sup>
Template C				
dATP	1.73 $\pm$ 0.24	140.4 $\pm$ 62.1	0.012	1.9 $\times$ 10 <sup>-3</sup>
dCTP	2.83 $\pm$ 0.24	224.8 $\pm$ 53.9	0.013	2.0 $\times$ 10 <sup>-3</sup>
dTTP	2.24 $\pm$ 0.30	174.6 $\pm$ 69.6	0.013	2.0 $\times$ 10 <sup>-3</sup>
dGTP	3.5 $\pm$ 0.16	0.55 $\pm$ 0.12	6.36	1
Template T				
dATP	3.25 $\pm$ 0.03	7.76 $\pm$ 0.23	0.42	1
dCTP	ND	ND	0.00030	7.1 $\times$ 10 <sup>-4</sup>
dTTP	0.20 $\pm$ 0.05	685.9 $\pm$ 309.3	0.00029	6.9 $\times$ 10 <sup>-4</sup>
dGTP	0.033 $\pm$ 0.004	74.6 $\pm$ 25.0	0.00044	1.0 $\times$ 10 <sup>-3</sup>
Template G				
dATP	0.11 $\pm$ 0.03	567.5 $\pm$ 457.7	0.00019	1.5 $\times$ 10 <sup>-3</sup>
dCTP	1.90 $\pm$ 0.17	14.8 $\pm$ 4.02	0.13	1
dTTP	ND	ND	0.000038	2.9 $\times$ 10 <sup>-4</sup>
dGTP	ND	ND	0.00027	2.1 $\times$ 10 <sup>-3</sup>

<sup>a</sup> DNA templates shown in Fig. 3A were used for kinetic analyses.

<sup>b</sup>  $f_{\text{inc}} = (V_{\max}/K_m)_{\text{incorrect}}/(V_{\max}/K_m)_{\text{correct}}$ .

<sup>c</sup> ND, not detected. The reaction velocity ( $v$ ) remained linear throughout the entire dNTP concentration range used (0 to 3,000  $\mu$ M). Therefore, individual  $V_{\max}$  and  $K_m$  values could not be determined based on the  $v$ -versus-[dNTP] plot. The  $V_{\max}/K_m$  value was determined by the slope of the initial velocity.

ern blot analysis using a mouse monoclonal antibody specific to the His<sub>6</sub> tag at its N terminus (Fig. 1B). The purified human Pol $\mu$  migrated as a 60-kDa protein on a sodium dodecyl sulfate (SDS)-10% polyacrylamide gel (Fig. 1A and B), consistent with its calculated molecular mass of 55 kDa. Separately, we deleted the C-terminal 83 amino acids of human Pol $\mu$  by gene deletion. Since the mutant protein (Pol $\mu$  $\Delta$ C83) lacks several conserved amino acid residues that are known to be critical for Pol $\beta$  activity (2, 8), Pol $\mu$  $\Delta$ C83 is expected to lose the polymerase activity. Using the same vector and under conditions identical to those with the wild-type human Pol $\mu$ , the His<sub>6</sub>-tagged Pol $\mu$  $\Delta$ C83 mutant protein was expressed in yeast cells and partially purified by an affinity Ni column. As indicated by Western blot analysis using the monoclonal antibody against the His<sub>6</sub> tag, the Pol $\mu$  $\Delta$ C83 protein migrated as a 48-kDa protein on an SDS-10% polyacrylamide gel (Fig. 1C), consistent with its calculated molecular mass of 45 kDa. Using similar amounts (as estimated from a Western blot analysis) of the Ni column fractions of Pol $\mu$  and Pol $\mu$  $\Delta$ C83, a DNA polymerase activity was readily detected with the wild-type Pol $\mu$  (Fig. 1D, lane 1) but was undetectable with the Pol $\mu$  $\Delta$ C8 mutant (Fig. 1D, lane 2). These results show that the DNA polymerase activity being studied is intrinsic to the purified human Pol $\mu$  rather than a contaminant DNA polymerase from yeast.

**Human Pol $\mu$  is a distributive polymerase that lacks a 3'  $\rightarrow$  5' proofreading exonuclease activity.** In a standard DNA polymerase assay, purified human Pol $\mu$  extended the <sup>32</sup>P-labeled 16-mer primer by 1 nucleotide in 2 min. With increasing reaction time, longer DNA strands were synthesized (Fig. 2A). However, DNA synthesis largely stopped after polymerizing only 6 nucleotides in 60 min (Fig. 2A, lane 6). When human Pol $\mu$  was increased by 20-fold (10-fold molar excess over the

template), only 9 nucleotides were polymerized in 10 min (data not shown). Thus, human Pol $\mu$  is a distributive polymerase and is capable of only short-stretch DNA synthesis. To examine the 3'  $\rightarrow$  5' proofreading exonuclease activity, we incubated human Pol $\mu$  with two DNA templates containing either a matched or a mismatched base pair at the primer 3' end (Fig. 2B). While the proofreading exonuclease activity of the Klenow fragment of *E. coli* DNA polymerase I was readily detected (Fig. 2B, lanes 2 and 5), human Pol $\mu$  did not degrade either the matched or the mismatched primers (Fig. 2B, lanes 3 and 6). These results show that human Pol $\mu$  does not possess a 3'  $\rightarrow$  5' proofreading exonuclease activity.

**DNA synthesis fidelity of human Pol $\mu$ .** To determine whether the biochemical properties of human Pol $\mu$  are consistent with a role in somatic hypermutation as speculated recently (8), we examined the DNA synthesis fidelity of this polymerase. Sequences from the JH4-JH5 intron of the rearranged human JH gene were chosen for analyzing Pol $\mu$  fidelity such that the results could be compared with the reported hypermutation spectrum (18). DNA polymerase assays with purified human Pol $\mu$  were performed in the presence of only one dNTP, using templates A, C, T, and G (Fig. 3A). Except for some G incorporation with the template A substrate (Fig. 3B, Temp A, lane 5), misincorporation by human Pol $\mu$  was not detectable in these sequence contexts (Fig. 3B).

To quantitatively measure DNA synthesis fidelity, we performed steady-state kinetic analyses of nucleotide incorporation by human Pol $\mu$ , using a method described by Creighton et al. (6). DNA polymerase assays were performed with increasing concentrations of a single dNTP using 14 fmol of purified human Pol $\mu$  and 50 fmol of the primed templates A, C, T, and G (Fig. 3A), respectively. Four kinetic parameters were ob-

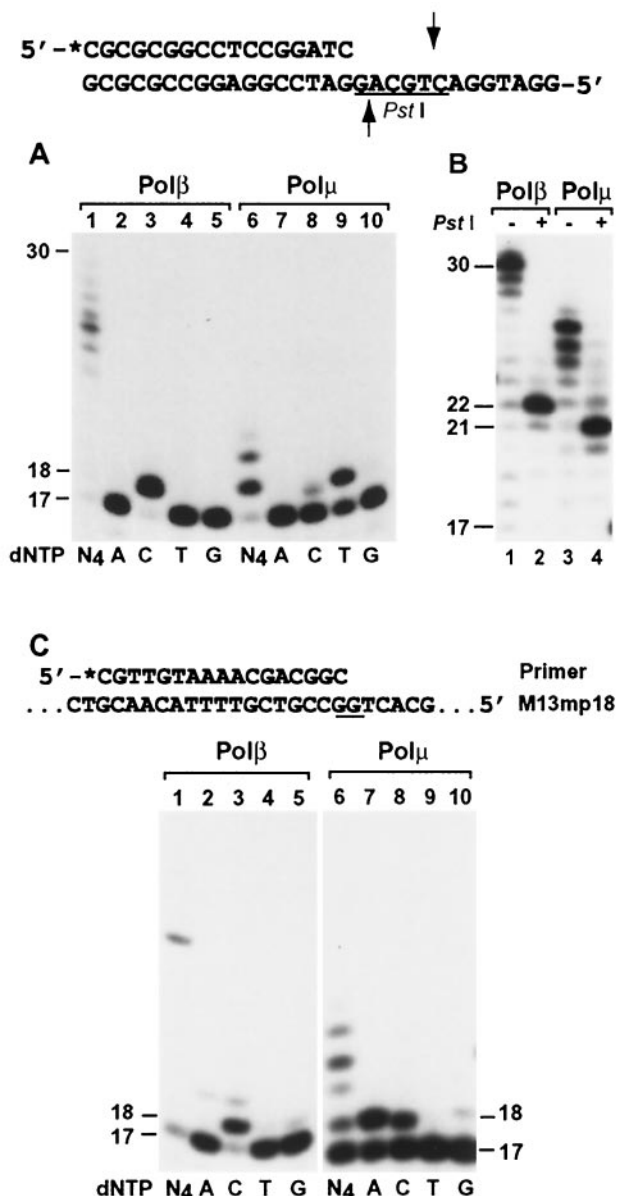


FIG. 4. Frameshift DNA synthesis at the template GG sequence by human Polμ. (A) Using the indicated DNA substrate, standard DNA polymerase assays were performed with human Polβ (23 ng; 605 fmol) or human Polμ (1.5 ng; 27 fmol) in the presence of a single dNTP (dATP [A], dCTP [C], dTTP [T], or dGTP [G]) or all four dNTPs (N<sub>4</sub>) as indicated. (B) Polymerase assays were performed at 37°C for 30 min, using human Polβ (23 ng; 605 fmol) or human Polμ (30 ng; 540 fmol) as indicated. After the polymerase reaction, 5 μl of the reaction products was mixed with 2 μl of H<sub>2</sub>O, 1 μl of the 10× *Pst*I buffer (500 mM Tris-HCl, pH 8.0, 100 mM MgCl<sub>2</sub>, and 500 mM NaCl), and 2 μl of *Pst*I (20 U). After incubation at 37°C for 4 h, the digested products were separated by electrophoresis on a 20% denaturing polyacrylamide gel and visualized by autoradiography. Samples without (-) or with (+) *Pst*I treatment are indicated. Underline, *Pst*I recognition sequence; arrows, *Pst*I cleavage sites. (C) Using single-stranded M13mp18 containing a 17-mer 5' <sup>32</sup>P-labeled (asterisk) primer, DNA polymerase assays were performed with human Polβ (23 ng; 605 fmol) or human Polμ (7.5 ng; 135 fmol) at 30°C for 10 min in the presence of a single dNTP or all four dNTPs as indicated. The analyzed template GG sequence is underlined. DNA size markers in nucleotides are indicated on the sides.

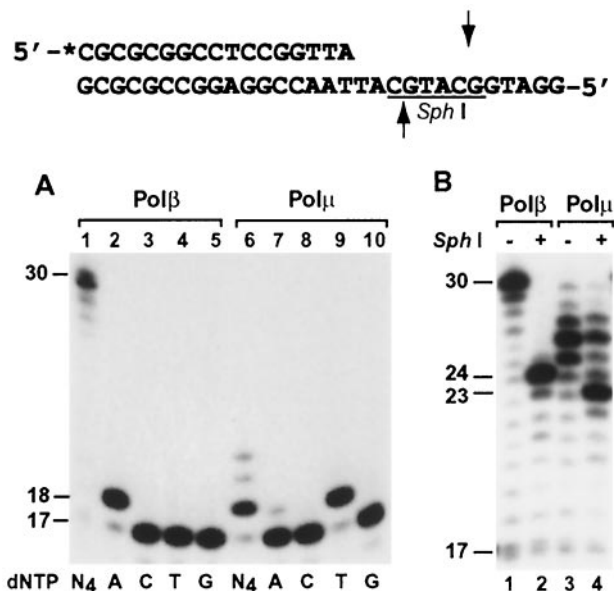


FIG. 5. Frameshift DNA synthesis at the template TT sequence by human Polμ. (A) Using the indicated DNA substrate, standard DNA polymerase assays were performed with human Polβ (23 ng; 605 fmol) or human Polμ (1.5 ng; 27 fmol) in the presence of a single dNTP (dATP [A], dCTP [C], dTTP [T], or dGTP [G]) or all four dNTPs (N<sub>4</sub>) as indicated. (B) Polymerase assays were performed at 37°C for 30 min, using human Polβ (23 ng; 605 fmol) or human Polμ (30 ng; 540 fmol) as indicated. After the polymerase reaction, 5 μl of the reaction products was mixed with 2 μl of H<sub>2</sub>O, 1 μl of the 10× *Sph*I buffer (100 mM Tris-HCl, pH 7.9, 100 mM MgCl<sub>2</sub>, 500 mM NaCl, and 10 mM dithiothreitol), and 2 μl of *Sph*I (10 U). After incubation at 37°C for 4 h, the digested products were separated by electrophoresis on a 20% denaturing polyacrylamide gel. Samples without (-) or with (+) *Sph*I treatment are indicated. DNA size markers in nucleotides are indicated on the left. Asterisk, <sup>32</sup>P label. Underline, *Sph*I recognition sequence; arrows, *Sph*I cleavage sites.

tained:  $V_{max}$ ,  $K_m$ ,  $V_{max}/K_m$ , and  $f_{inc}$  (Table 1). As indicated by the  $V_{max}/K_m$  values, human Polμ activity is most efficient opposite template C and much less efficient opposite the other three template bases (Table 1). The fidelity of nucleotide incorporation is indicated by the  $(V_{max}/K_m)_{incorrect}/(V_{max}/K_m)_{correct}$  values ( $f_{inc}$ ) (6). Except for G incorporation with the template A substrate, the misincorporation error rates ( $f_{inc}$ ) of human Polμ were not exceptionally high (Table 1) compared to those of human DNA polymerases η, ι, and κ (14, 15, 19, 23, 28, 38, 39). Furthermore, the Polμ specificity of misincorporations at the examined A, C, T, and G sites were generally inconsistent with the reported hypermutation specificity at the corresponding sites of the human JH4-JH5 intron (18).

To further examine whether human Polμ is indeed prone to G misincorporation opposite template A, we performed the analysis again with a different template, 3'-GCCGAGGCC AATCATACAAGCTTAC-5' (the analyzed template A is underlined). In this sequence context, G, A, or C incorporations were not detected (data not shown). This and other experiments (see below) led us to infer that the G incorporation with the template A substrate shown in Fig. 3B is probably a result of -1 frameshift DNA synthesis opposite template C 2 nucleotides downstream rather than misincorporation opposite template A.

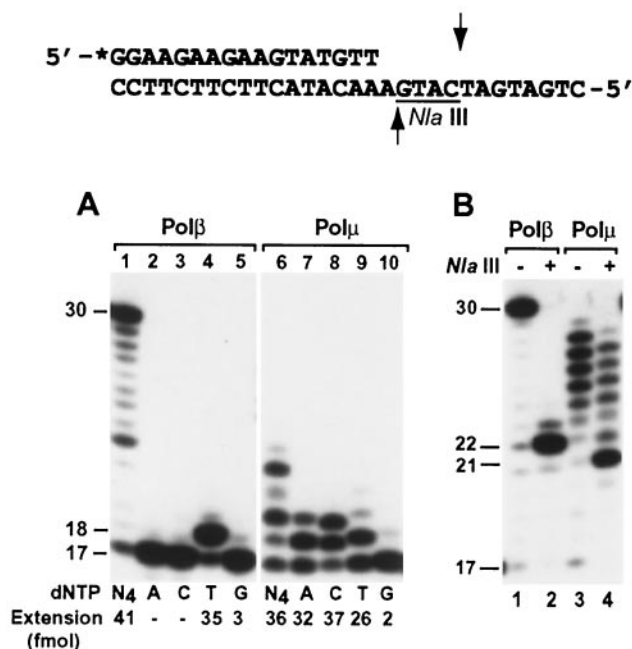


FIG. 6. Frameshift DNA synthesis at the template AA sequence by human Polμ. (A) Using the indicated DNA substrate, standard DNA polymerase assays were performed with human Polβ (23 ng; 605 fmol) or human Polμ (1.5 ng; 27 fmol) in the presence of a single dNTP (dATP [A], dCTP [C], dTTP [T], or dGTP [G]) or all four dNTPs (N<sub>4</sub>) as indicated. Quantitation of extended primers is shown below the gels. (B) Polymerase assays were performed at 37°C for 30 min, using human Polβ (23 ng; 605 fmol) or human Polμ (30 ng; 540 fmol) as indicated. After the polymerase reaction, 5 μl of the reaction products was mixed with 2 μl of H<sub>2</sub>O, 1 μl of the 10× *Nla*III buffer (200 mM Tris-acetate, pH 8.0, 100 mM MgCl<sub>2</sub>, 500 mM potassium acetate, and 10 mM dithiothreitol), and 2 μl of *Nla*III (20 U). After incubation at 37°C for 4 h, the digested products were separated by electrophoresis on a 20% denaturing polyacrylamide gel. Samples without (-) or with (+) *Nla*III treatment are indicated. DNA size markers in nucleotides are indicated on the left. Asterisk, <sup>32</sup>P label; underline, *Nla*III recognition sequence; arrows, *Nla*III cleavage sites.

**Frequent frameshift DNA synthesis by human Polμ.** We consistently observed that the DNA synthesis fidelity and nucleotide incorporation specificity of human Polμ were strongly influenced by the sequence context, with the single-nucleotide repeat sequences having the most dramatic effect. These observations led us to suspect that human Polμ may be especially prone to frameshift DNA synthesis in many sequence contexts. To directly examine this possibility, we analyzed DNA synthesis by human Polμ from template GG, TT, AA, and CC sequences.

A labeled 17-mer primer was annealed to the template GG, in which the primer 3' end was paired to the 3' G of the GG sequence (Fig. 4A and B). Normal DNA synthesis would lead to C incorporation, as observed with Polβ-catalyzed DNA synthesis (Fig. 4A, lanes 1 to 5). Misaligning the primer 3' C to the next template G would result in T incorporation and -1 frameshift DNA synthesis. As shown in Fig. 4A (lanes 6 to 10), human Polμ predominantly incorporated T. With higher Polμ concentration and extended incubation time, longer DNA strands were synthesized by human Polμ (Fig. 4B, lane 3), allowing us to examine the synthesis products by *Pst*I restriction digestion. Normal DNA synthesis would yield a 22-mer

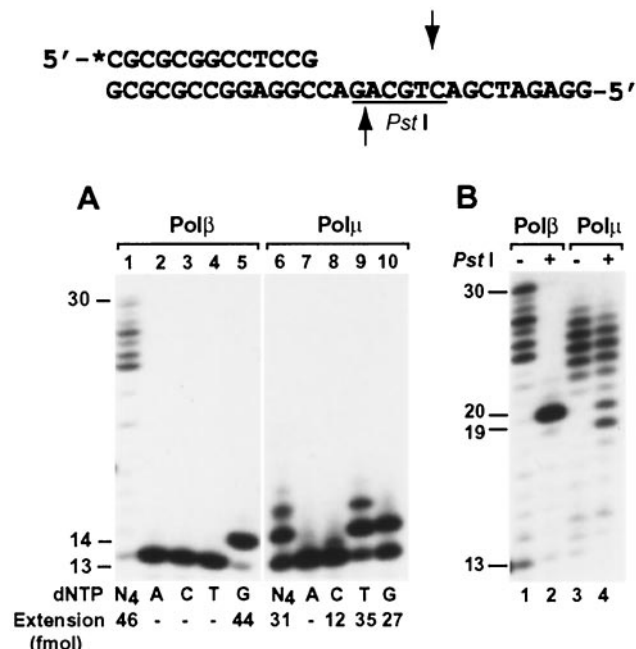


FIG. 7. Frameshift DNA synthesis at the template TT sequence by human Polμ. (A) Using the indicated DNA substrate, standard DNA polymerase assays were performed with human Polβ (23 ng; 605 fmol) or human Polμ (1.5 ng; 27 fmol) in the presence of a single dNTP (dATP [A], dCTP [C], dTTP [T], or dGTP [G]) or all four dNTPs (N<sub>4</sub>) as indicated. Quantitation of extended primers is shown below the gels. (B) Polymerase assays were performed at 37°C for 30 min, using human Polβ (23 ng; 605 fmol) or human Polμ (30 ng; 540 fmol) as indicated. After the polymerase reaction, 5 μl of the reaction products was treated with 20 U of *Pst*I as for Fig. 4B. The digested products were separated by electrophoresis on a 20% denaturing polyacrylamide gel. Samples without (-) or with (+) *Pst*I treatment are indicated. DNA size markers in nucleotides are indicated on the left. Asterisk, <sup>32</sup>P label; underline, *Pst*I recognition sequence; arrows, *Pst*I cleavage sites.

<sup>32</sup>P-labeled DNA fragment after the *Pst*I cleavage, as was observed with human Polβ-catalyzed DNA synthesis (Fig. 4B, lane 2). With Polμ-catalyzed DNA synthesis, the *Pst*I cleavage yielded a major 21-mer DNA fragment (Fig. 4B, lane 4). These results demonstrate that DNA synthesis by human Polμ at the examined template GG sequence is mediated predominantly by a -1 frameshift mechanism.

To determine whether this surprising result reflects an artificial short DNA template, which may be structurally more flexible, or reflects an intrinsic biochemical property of human Polμ, we performed DNA synthesis at the GG sequence using single-stranded M13mp18 circular DNA (7,249 bases) as the DNA template (Fig. 4C). As expected, human Polβ incorporated a C opposite the 5' G of the GG sequence (Fig. 4C, lanes 1 to 5). In contrast, -1 frameshift DNA synthesis would incorporate an A opposite the template T 5' to the GG sequence (Fig. 4C). Again, human Polμ most frequently incorporated an A (53% primer extension) and less frequently incorporated the correct C (39% primer extension) (Fig. 4C, lanes 6 to 10), indicating that DNA synthesis at the template GG sequence was mediated mainly by a -1 frameshift mechanism. In the presence of all four dNTPs (Fig. 4C, lane 6), nucleotide se-

TABLE 2. Kinetic measurement of  $-1$  frameshift DNA synthesis by human Pol $\mu$ <sup>a</sup>

dNTP	$V_{\max}$ (fmol/min; mean $\pm$ SD)	$K_m$ ( $\mu$ M; mean $\pm$ SD)	$V_{\max}/K_m$	Relative rate <sup>b</sup>
Template GG				
dCTP	1.44 $\pm$ 0.13	135.3 $\pm$ 39.4	0.011	1
dTTP	4.76 $\pm$ 0.18	21.8 $\pm$ 2.37	0.22	20
Template TT				
dATP	1.96 $\pm$ 0.02	42.6 $\pm$ 1.87	0.046	1
dTTP	3.12 $\pm$ 0.08	2.46 $\pm$ 0.28	1.27	28
Template AA				
dTTP	2.86 $\pm$ 0.08	58.3 $\pm$ 6.37	0.049	1
dCTP	2.91 $\pm$ 0.09	12.7 $\pm$ 1.22	0.23	4.7
Template CC				
dGTP	4.36 $\pm$ 0.14	13.7 $\pm$ 1.8	0.32	1
dTTP	4.72 $\pm$ 0.09	6.10 $\pm$ 0.46	0.77	2.4

<sup>a</sup> DNA templates GG, TT, AA, and CC (Fig. 4A, 5, 6, and 7, respectively) were used for kinetic analyses.

<sup>b</sup> For each template, incorporation of the correct nucleotide reflects normal DNA synthesis, whereas incorporation of the other nucleotide reflects  $-1$  frameshift DNA synthesis. Relative rate =  $(V_{\max}/K_m)_{-1\text{frameshift}}/(V_{\max}/K_m)_{\text{correct}}$ .

quence synthesized by human Pol $\mu$  is consistent with 5'-AGTG (the  $-1$  deletion product), based on the migration pattern of the DNA bands (mobility from fastest to slowest, C>A>T>G). Therefore, we conclude that the unprecedentedly high frequency of  $-1$  frameshift DNA synthesis at the template GG sequence is an intrinsic property of human Pol $\mu$ .

At the template TT sequence (Fig. 5), human Pol $\beta$  incorporated an A opposite the 5' T, as expected for normal DNA synthesis (Fig. 5A, lanes 1 to 5). The  $-1$  frameshift DNA synthesis would lead to T incorporation opposite the template A 5' to the TT sequence (Fig. 5). As shown in Fig. 5A (lanes 6 to 10), human Pol $\mu$  predominantly incorporated T. Remarkably, the correct A incorporation by human Pol $\mu$  had become barely detectable (Fig. 5A, lane 7). Cleavage of the synthesized DNA products by *SphI* restriction endonuclease would yield a <sup>32</sup>P-labeled 24-mer DNA fragment, as was observed with human Pol $\beta$ -catalyzed DNA synthesis (Fig. 5B, lane 2). With Pol $\mu$ -catalyzed DNA synthesis, the *SphI* cleavage yielded a major 23-mer DNA fragment (Fig. 5B, lane 4). Pol $\mu$ -synthesized products were less efficiently cleaved by *SphI* (Fig. 5B, compare lanes 2 and 4), probably due to shorter DNA strands and/or the 1-nucleotide loop on the template strand. These results show that DNA synthesis by human Pol $\mu$  at the examined template TT sequence is mediated predominantly by a  $-1$  frameshift mechanism.

At the template AA sequence (Fig. 6), human Pol $\beta$  incorporated a T opposite the 5' A, as expected for normal DNA synthesis (Fig. 6A, lanes 1 to 5). The  $-1$  frameshift DNA synthesis would lead to C incorporation opposite the template G 5' to the AA sequence (Fig. 6). As shown in Fig. 6A (lanes 6 to 10), human Pol $\mu$  most frequently incorporated C. Less frequently, A could also be incorporated by human Pol $\mu$  (Fig. 6B, lane 7), which most likely resulted from  $-2$  frameshift DNA synthesis by using the template T 3 nucleotides downstream of the primer 3' end. Cleavage of the Pol $\beta$ -synthesized products with *NlaIII* restriction endonuclease yielded a major 22-mer DNA band (Fig. 6B, lane 2), as expected for normal DNA synthesis. In contrast, identical treatment of the Pol $\mu$ -synthesized products with *NlaIII* yielded a major 21-mer DNA band (Fig. 6B, lane 4). The less efficient cleavage of Pol $\mu$ -synthesized products by *NlaIII* (Fig. 6B, compare lanes 2 and

4) was probably due to shorter DNA strands; the 1-nucleotide loop on the template strand;  $-2$  frameshift DNA synthesis, which would destroy the *NlaIII* recognition site; or combinations of these factors. These results show that DNA synthesis by human Pol $\mu$  at the examined template AA sequence is mediated predominantly by a  $-1$  frameshift mechanism.

At the template CC sequence (Fig. 7), human Pol $\beta$  incorporated a G opposite the 5' C, as expected for normal DNA synthesis (Fig. 7A, lanes 1 to 5). The  $-1$  frameshift DNA synthesis would lead to T incorporation opposite the template A 5' to the CC sequence (Fig. 7). As shown in Fig. 7A (lanes 6 to 10), human Pol $\mu$  favored T incorporation over the correct G incorporation. Minor C incorporation was also observed (Fig. 7A, lane 8), which most likely resulted from  $-2$  frameshift DNA synthesis by using the template G 3 nucleotides downstream of the primer 3' end. Cleavage of the Pol $\beta$ -synthesized products with the *PstI* restriction endonuclease yielded a major 20-mer DNA band (Fig. 7B, lane 2), as expected for normal DNA synthesis. In contrast, following *PstI* cleavage of the Pol $\mu$ -synthesized products, 1.3-fold more 19-mer DNA band than 20-mer DNA band was formed (Fig. 7B, lane 4). *PstI* cleavage of Pol $\mu$ -synthesized products was significantly less efficient than that of Pol $\beta$ -synthesized products (Fig. 7B, compare lanes 2 and 4). The precise cause of this difference is not known. Possible factors include shorter DNA strands, the 1-nucleotide loop on the template strand, some  $-2$  frameshift DNA synthesis, or combinations of these. These results show that human Pol $\mu$  prefers  $-1$  frameshift DNA synthesis to normal DNA synthesis at the examined template CC sequence.

As indicated by the steady-state kinetic values (Table 2), the rate of  $-1$  frameshift synthesis by human Pol $\mu$  was 20-, 28-, 4.7-, and 2.4-fold higher than normal DNA synthesis at the GG, TT, AA, and CC sequences, respectively, in the sequence contexts examined. Together, these results show that human Pol $\mu$  catalyzes highly frequent frameshift DNA synthesis, which can predominate as the major DNA synthesis mechanism in some sequence contexts.

**Mismatch extension by human Pol $\mu$ .** Without a 3'  $\rightarrow$  5' proofreading exonuclease activity, human Pol $\mu$  cannot remove mismatched nucleotides at the primer 3' end. To examine

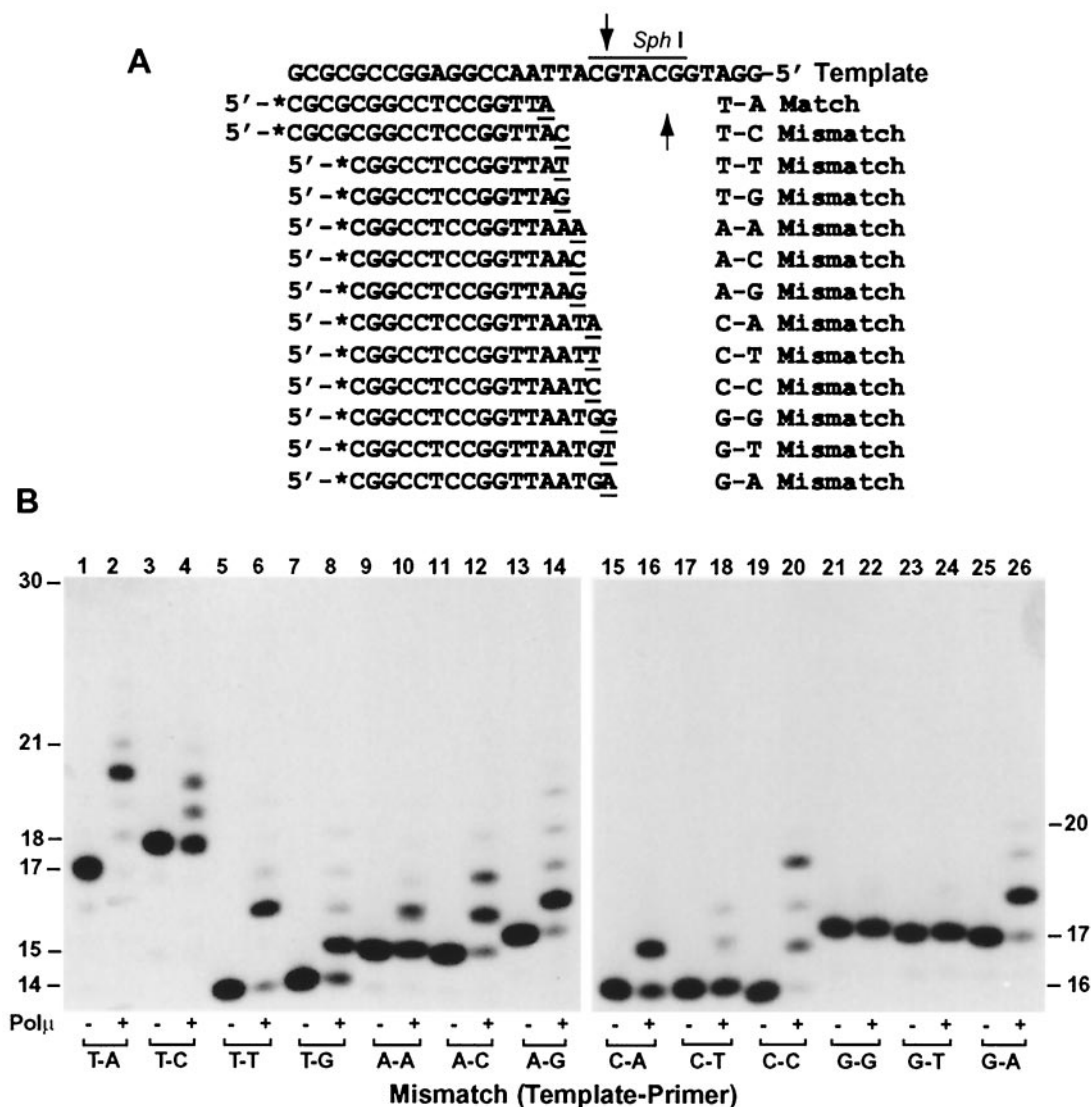


FIG. 8. Mismatch extensions by human Pol $\mu$ . (A) Various primers labeled at their 5' ends with  $^{32}$ P (asterisks) were annealed to the indicated template, generating 12 possible mismatches at the primer 3' ends. One normal T-A-matched substrate was used as the control. The *Sph*I recognition sequence is overlined, and the mismatched primer 3' ends are underlined. Arrows, *Sph*I cleavage sites. (B) Matched and mismatched substrates were incubated with (+) or without (-) human Pol $\mu$  (3 ng; 54 fmol) under standard polymerase assay conditions. DNA size markers in nucleotides are indicated on the sides.

mismatch extension activity of human Pol $\mu$ , we performed primer extension assays using the 12 possible base pair mismatches (Fig. 8A). As shown in Fig. 8B, except for G-G, and G-T (template-primer), all other mismatches were extended by human Pol $\mu$ . T-T, A-G, C-C, and G-A mismatches were extended most efficiently (Fig. 8B, lanes 6, 14, 20, and 26).

To identify nucleotides incorporated during mismatch extension, we performed the extension assays again in the presence of only one dNTP. Human Pol $\mu$  incorporated G with the T-T mismatch (Fig. 9, lanes 1 to 5), C with the A-G mismatch (Fig. 9, lanes 16 to 20), and T with the G-A mismatch (Fig. 9, lanes 31 to 35). These incorporations are precisely predicted by a -1 frameshift synthesis mechanism involving misaligning the primer 3' end with the next complementary template base prior to DNA synthesis. Human Pol $\mu$  incorporated C with the

T-G mismatch (Fig. 9, lanes 6 to 10) and T with the C-A mismatch (Fig. 9, lanes 21 to 25), which are predicted by a -2 frameshift synthesis mechanism involving misaligning the primer 3' end with the complementary template base 2 nucleotides downstream prior to DNA synthesis. With the A-C mismatch, human Pol $\mu$  preferentially incorporated A (Fig. 9, lane 12) and less frequently C (Fig. 9, lane 13), which was consistent with -2 frameshift synthesis by misaligning the primer 3' C 2 nucleotides downstream with the template G and -1 frameshift synthesis using the template G 2 nucleotides downstream, respectively. With the C-C mismatch, human Pol $\mu$  slightly preferred A incorporation over T incorporation, consistent with misaligning the primer 3' C with the next template G as the preferred event prior to DNA synthesis (-1 frameshift) (Fig. 9, lanes 26 to 30). T incorporation (Fig. 9,



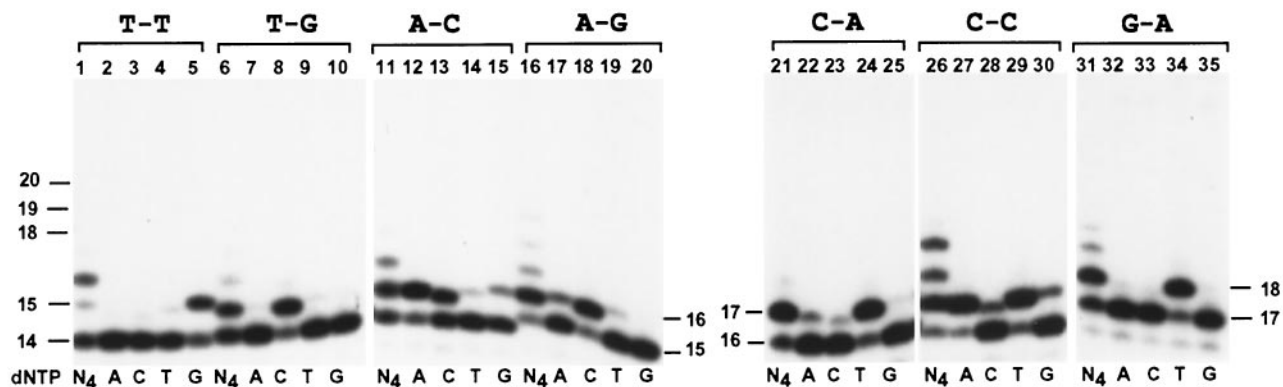


FIG. 9. Nucleotide incorporation during mismatch extension. Using the mismatched DNA substrates as indicated (sequences shown in Fig. 8A), mismatch extension was performed with 3 ng (54 fmol) of human Pol $\mu$  under standard polymerase assay conditions. The reactions were carried out using a single dNTP (dATP [A], dCTP [C], dTTP [T], or dGTP [G]) or all four dNTPs (N<sub>4</sub>) as indicated. DNA size markers in nucleotides are indicated on the sides.

lane 29) was consistent with  $-2$  frameshift DNA synthesis using the template A 3 nucleotides downstream.

To test the notion that mismatch extension by human Pol $\mu$  is mediated mainly by frameshift DNA synthesis, we slightly modified the DNA template and analyzed extensions from G-G and G-A mismatches. The template 3'-TA-5' sequence immediately downstream of the mismatch was replaced by 3'-CT-5' (Fig. 10A). Frameshift extension predicts that human Pol $\mu$  should then be able to extend the G-G mismatch that was refractory to extension in the original sequence context (Fig. 8), since the primer 3' G can pair with the next template C. Furthermore, A incorporation is predicted. As shown in Fig. 10A (lanes 1 to 5), the G-G mismatch was indeed effectively extended by human Pol $\mu$ , and A was incorporated. In contrast, the G-A mismatch extension by human Pol $\mu$  was drastically reduced in the new sequence context (Fig. 10A, lanes 6 to 10).

Similar to the paired T-A extension (Fig. 8B, lane 2), human Pol $\mu$  extended the mismatched primers by only 1 or a few nucleotides under the reaction conditions of low enzyme concentration and short incubation time (Fig. 8B). With higher Pol $\mu$  concentration and extended incubation time, longer DNA strands were synthesized from a mismatched primer 3' end (Fig. 10B, lanes 1, 3, and 5), which allowed us to analyze the Pol $\mu$ -synthesized products by *Sph*I restriction digestion. After *Sph*I cleavage, a 20-mer <sup>32</sup>P-labeled DNA fragment is expected for extension without deletion. As shown in Fig. 10B (lanes 2 and 6), *Sph*I cleavage of the Pol $\mu$ -catalyzed T-T and A-G extension products yielded a major 19-mer DNA fragment, demonstrating  $-1$  deletion as the major DNA product. *Sph*I cleavage of the Pol $\mu$ -catalyzed T-G extension products yielded a major 18-mer DNA fragment (Fig. 10B, lane 4), demonstrating  $-2$  deletion as the major DNA product. Together, these results show that human Pol $\mu$  can efficiently extend base mismatches by frameshift DNA synthesis.

**Human Pol $\mu$  promotes microhomology search and microhomology pairing in DNA.** The unprecedented ability of human Pol $\mu$  to perform frameshift DNA synthesis led us to suspect that this polymerase may be capable of promoting microhomology search by realigning two strands of DNA. To test this hypothesis, we prepared a DNA template to which

three <sup>32</sup>P-labeled primers were separately annealed. The resulting DNA substrates contained 2-, 3-, and 4-base mismatches, respectively, at the primer 3' end (Fig. 11A). Up to 3-nucleotide microhomology was incorporated in the template DNA 2 nucleotides downstream from the primer 3' end. Human Pol $\mu$  was then incubated with the DNA substrates under polymerase reaction conditions. If human Pol $\mu$  is able to promote homology search by realigning the template and the primer strands of DNA, DNA synthesis is expected and C incorporation is predicted. Indeed, DNA synthesis was observed and C was predominantly incorporated in every case (Fig. 11A, lanes 3, 8, and 13). Minor T incorporation was also observed with substrates containing two or three mismatches (Fig. 11A, lanes 4 and 9), probably as a result of mismatch extension without frameshift. Increasing mismatched bases from two to four at the primer 3' end greatly decreased T incorporation by human Pol $\mu$  (Fig. 11A, lanes 11 to 15), suggesting more efficient microhomology pairing with increasing mismatches at the primer 3' end.

To examine whether the mismatched primer end can pair with a microhomologous region further downstream in the template, we modified the template sequence such that the last 2 nucleotides (5'-TG-3') of the primer were complementary to two template 3'-AC-5' sequences located 4 and 6 nucleotides, respectively, downstream (Fig. 11B). If microhomology pairing had occurred at the first template 3'-AC-5' sequence 4 nucleotides away, human Pol $\mu$  would incorporate a T. If microhomology pairing had occurred at the second template 3'-AC-5' sequence 6 nucleotides away, human Pol $\mu$  would incorporate a C. As predicted by such microhomology pairings, T incorporation by human Pol $\mu$  was observed (Fig. 11B, lane 9), and less frequently, C incorporation was also observed (Fig. 11B, lane 8). A incorporation that would have resulted from primer extension without frameshift was not detected (Fig. 11B, lane 7). In contrast, human Pol $\beta$  (even in greatly excessive amounts) was completely unresponsive to this DNA substrate (Fig. 11, lanes 1 to 5). These results show that human Pol $\mu$  is capable of promoting microhomology search and subsequent microhomology pairing in DNA.

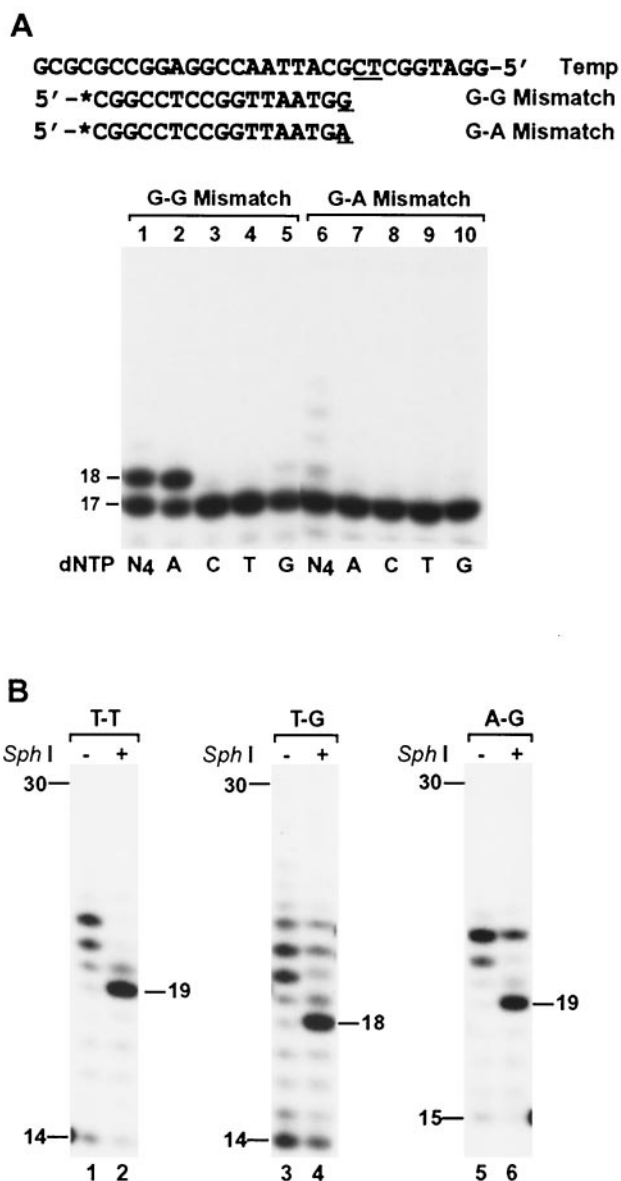


FIG. 10. Evidence that mismatch extension by human Pol $\mu$  is mainly mediated by frameshift DNA synthesis. (A) The template sequence of Fig. 8A was slightly modified such that the template 3'-T A-5' immediately downstream of the G-G and G-A mismatches was replaced by 3'-CT-5' (underlined). These mismatched DNA substrates were analyzed for extension by 3 ng (54 fmol) of human Pol $\mu$  using a single dNTP (dATP [A], dCTP [C], dTTP [T], or dGTP [G]) or all four dNTPs (N<sub>4</sub>) as indicated. The mismatched primer 3' and A are underlined. Asterisk, <sup>32</sup>P label. (B) Polymerase assays were performed with human Pol $\mu$  (30 ng; 540 fmol) at 37°C for 30 min. After the polymerase reaction, 5  $\mu$ l of the reaction products was treated with 10 U of *Sph*I as for Fig. 5B. The digested products were separated by electrophoresis on a 20% denaturing polyacrylamide gel. Samples without (-) or with (+) *Sph*I treatment are indicated. DNA size markers in nucleotides are indicated on the sides. Mismatched DNA sequences are shown in Fig. 8A.

## DISCUSSION

To facilitate understanding of the biological function of human DNA Pol $\mu$ , we have purified this polymerase and ana-

lyzed its biochemical properties. Surprisingly, human Pol $\mu$  catalyzes frameshift DNA synthesis with an unprecedentedly high frequency. The rate of frameshift DNA synthesis is greatly dependent on the sequence context of the template base to be copied. When the primer 3' end is complementary to the next template base (template AA, TT, GG, and CC sequences), human Pol $\mu$  most efficiently misaligns the primer end to the next template base prior to DNA synthesis, resulting in -1 deletion products. Remarkably, at the template AA, TT, GG, and CC sequences examined in this study, -1 frameshift synthesis has become the predominant mechanism of DNA synthesis by human Pol $\mu$ , with rates ranging from 2.4- to 28-fold higher than the normal DNA synthesis. When the primer 3' end is complementary to the template base 2 nucleotides downstream, human Pol $\mu$  can often efficiently catalyze -2 primer-template misalignment prior to DNA synthesis, leading to -2 deletion (data not shown). Compared to template AA, TT, and GG sequences, frameshift DNA synthesis opposite template CC is less efficient, which seems to be inversely correlated to the relatively higher catalytic efficiency of human Pol $\mu$  opposite template C. We have additionally examined DNA templates in which the primer end could be misaligned backward to "loop out" the primer. DNA synthesis based on such a mechanism would produce insertion products. However, under the conditions used in this study, there was no evidence supporting such an insertion frameshift DNA synthesis by human Pol $\mu$  (data not shown).

Recently, Dominguez et al. (8) proposed that human Pol $\mu$  might function as a DNA mutator polymerase in somatic hypermutation of immunoglobulin genes. Extensive analyses of immunoglobulin gene mutations have indicated that hypermutation mainly results in base substitutions (point mutations) (4, 12). Thus, a major hypermutation DNA polymerase must satisfy at least two biochemical requirements: (i) be highly error prone and (ii) have higher base substitution rates than frameshift DNA synthesis rates. Using DNA sequences derived from the JH4-JH5 intron of the rearranged human JH gene, the measured error rates of human Pol $\mu$  are not exceptionally high (Table 1). Except for G incorporation with template A, which may result from -1 frameshift DNA synthesis, all other error rates most likely reflect the base substitution rates of human Pol $\mu$ . These error rates suggest that human Pol $\mu$  is significantly more accurate than human DNA polymerases  $\eta$ ,  $\iota$ , and  $\kappa$  with respect to base substitutions during DNA synthesis (14, 15, 19, 23, 28, 38, 39). In contrast, the extraordinary ability of human Pol $\mu$  to perform frameshift DNA synthesis is unmatched by any other DNA polymerases known. The hypermutation spectrum at the JH4-JH5 intron sequence shows base substitution as the vast majority of mutations (18). Among the 242 mutations observed, -1 deletion was scored only once, although more than one single-nucleotide repeat sequence is contained within every 10 bp of the JH4-JH5 intron (18). Since an intron sequence was analyzed, the hypermutation spectrum reported by Levy et al. (18) could not have been biased by selection. Clearly, the biochemical property of prevalent frameshift DNA synthesis has ruled out human Pol $\mu$  as a significant somatic hypermutation DNA polymerase. DNA Pol $\iota$  appears to be a more likely candidate for somatic hypermutation, as originally proposed by us (38) and by Tissier et al. (28).

What, then, is the cellular function of human Pol $\mu$ ? Our

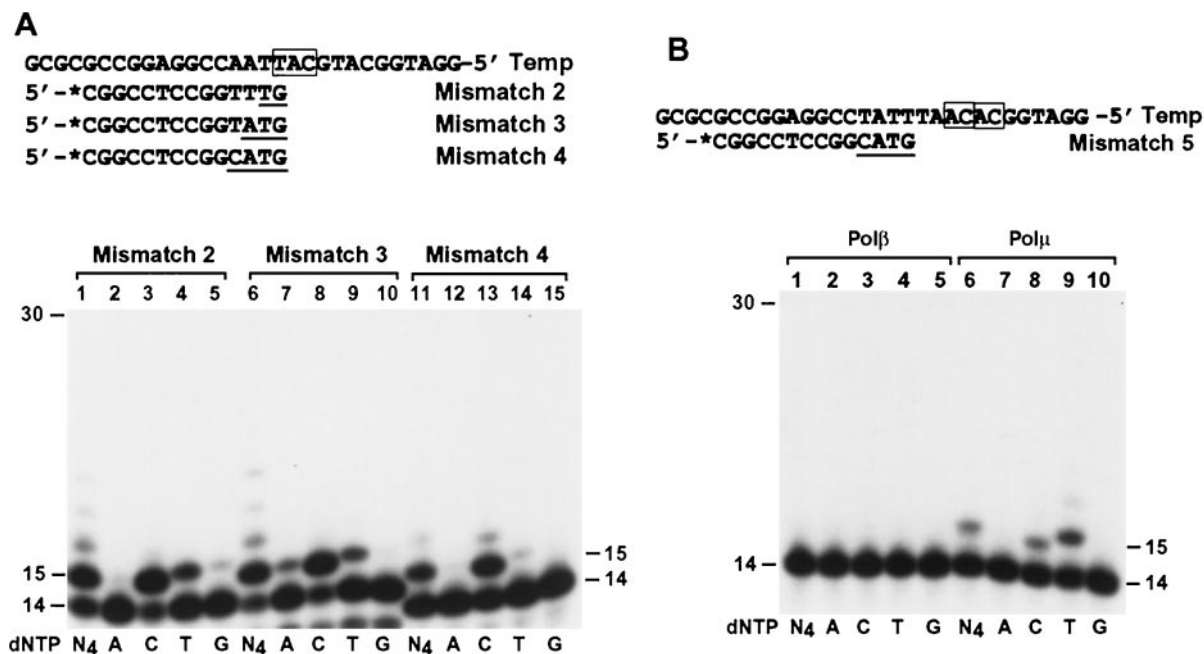


FIG. 11. Microhomology search and microhomology pairing promoted by human Pol $\mu$ . (A) A DNA template was separately annealed to three  $^{32}$ P-labeled (asterisks) 14-mer primers as shown, forming two, three, and four mismatches (underlined), respectively, at the primer ends. A sequence of 2 or 3 nucleotides (boxed) that could pair with the last 2 or 3 nucleotides of the primers was contained in the template 2 nucleotides downstream. (B) A  $^{32}$ P-labeled 14-mer primer was annealed to a template as shown, forming 4-nucleotide mismatches at the primer 3' end (underlined). Two 3'-AC-5' sequences located 4 and 6 nucleotides, respectively, downstream in the template (boxed) were complementary to the last 2 nucleotides of the primer. These DNA substrates were incubated with human Pol $\beta$  (23 ng; 605 fmol) or human Pol $\mu$  (3 ng; 54 fmol) under standard DNA polymerase assay conditions in the presence of a single dNTP (dATP [A], dCTP [C], dTTP [T], or dGTP [G]) or all four dNTPs as indicated. DNA size markers in nucleotides are indicated on the sides.

biochemical studies may provide an important clue to the answer. Human Pol $\mu$  is highly capable of realigning the primer and the template strands of DNA. Such realignment of two DNA strands is especially prominent at a mismatched primer end. Primer ends that contain one to four of the mismatches examined all promote Pol $\mu$ -mediated DNA strand realignment. The result of the primer-template realignment is microhomology pairing between the primer end and the template strand downstream. Therefore, human Pol $\mu$  is able to promote microhomology search and subsequent microhomology pairing between the primer strand and the template strand of DNA. Following microhomology pairing (1- to 3-base pairing), human Pol $\mu$  can extend the primer end by 1 or a few nucleotides, consequently further stabilizing the DNA strand realignment and the paired microhomology region. The ability of human Pol $\mu$  to promote microhomology search and microhomology pairing between the primer and the template strands of DNA strongly suggests a function for this polymerase in NHEJ during repair of double-strand DNA breaks. Several proteins have been identified for NHEJ, including Ku70, Ku80, DNA-PK<sub>cs</sub>, XRCC4, and DNA ligase IV (25). It is believed that the Ku70-Ku80 heterodimer binds to the DNA ends and holds the ends together (7, 25). The XRCC4-ligase IV complex is believed to be required to ligate DNA strands at the last step of NHEJ (7, 11, 34). A DNA polymerase has not been identified for NHEJ in higher eukaryotes, although NHEJ would conceptually require a DNA polymerase activity. We propose that human Pol $\mu$  plays an important role in NHEJ. We hypothesize that

human Pol $\mu$  may function to promote microhomology search and microhomology pairing during NHEJ. Subsequent DNA polymerase activity of Pol $\mu$  would stabilize the microhomology pairing to prepare the XRCC4-ligase IV complex for DNA ligation.

In addition to repairing damage-induced double-strand DNA breaks, NHEJ is also an essential mechanism of the V(D)J recombination. V(D)J recombination helps generate diversity of antigen-binding sites of antibodies and T-cell receptor proteins during lymphoid cell development. A role for Pol $\mu$  in NHEJ would predict that this polymerase is important for V(D)J recombination in lymphoid cells. Ubiquitous expression of human Pol $\mu$  in various tissues, including lymphoid tissues (1, 8), is consistent with a role of this polymerase in NHEJ and V(D)J recombination. Recently, Wilson and Lieber (35) reported evidence suggesting that yeast Pol4 (Pol $\beta$ ) is involved in NHEJ. Since yeast Pol4 appears to be more related to human Pol $\lambda$  and Pol $\mu$  than to human Pol $\beta$  (1), the results of Wilson and Lieber (35) support our model in which Pol $\mu$  functions in NHEJ. As proposed most recently by Ruiz et al. (26), an 8-kDa domain with potential DNA-binding activity and an N-terminal BRCT domain similar to that of the TdT in human Pol $\mu$  are consistent with a role of this polymerase in NHEJ and V(D)J recombination.

#### ACKNOWLEDGMENTS

This work was supported by a New Investigator Award in Toxicology from the Burroughs Wellcome Fund and research grant CA67978 from NIH.

## REFERENCES

1. Aoufouchi, S., E. Flatter, A. Dahan, A. Faili, B. Bertocci, S. Storck, F. Delbos, L. Cocea, N. Gupta, J. C. Weill, and C. A. Reynaud. 2000. Two novel human and mouse DNA polymerases of the polX family. *Nucleic Acids Res.* **28**:3684–3693.
2. Beard, W. A., and S. H. Wilson. 2000. Structural design of a eukaryotic DNA repair polymerase: DNA polymerase  $\beta$ . *Mutat. Res.* **460**:231–244.
3. Bentolila, L. A., M. Fanton d'Andon, Q. T. Nguyen, O. Martinez, F. Rougeon, and N. Doyen. 1995. The two isoforms of mouse terminal deoxynucleotidyl transferase differ in both the ability to add N regions and subcellular localization. *EMBO J.* **14**:4221–4229.
4. Bertocci, B., L. Quint, F. Delbos, C. Garcia, C. A. Reynaud, and J. C. Weill. 1998. Probing immunoglobulin gene hypermutation with microsatellites suggests a nonreplicative short patch DNA synthesis process. *Immunity* **9**:257–265.
5. Chang, L. M., and F. J. BOLLUM. 1986. Molecular biology of terminal transferase. *Crit. Rev. Biochem.* **21**:27–52.
6. Creighton, S., L. B. Bloom, and M. F. Goodman. 1995. Gel fidelity assay measuring nucleotide misinsertion, exonucleolytic proofreading, and lesion bypass efficiencies. *Methods Enzymol.* **262**:232–256.
7. Critchlow, S. E., and S. P. Jackson. 1998. DNA end-joining: from yeast to man. *Trends Biochem. Sci.* **23**:394–398.
8. Dominguez, O., J. F. Ruiz, T. Lain de Lera, M. Garcia-Diaz, M. A. Gonzalez, T. Kirchhoff, A. C. Martinez, A. Bernad, and L. Blanco. 2000. DNA polymerase mu (Pol  $\mu$ ), homologous to TdT, could act as a DNA mutator in eukaryotic cells. *EMBO J.* **19**:1731–1742.
9. Friedberg, E. C., W. J. Feaver, and V. L. Gerlach. 2000. The many faces of DNA polymerases: strategies for mutagenesis and for mutational avoidance. *Proc. Natl. Acad. Sci. USA* **97**:5681–5683.
10. Garcia-Diaz, M., O. Dominguez, L. A. Lopez-Fernandez, L. T. de Lera, M. L. Saniger, J. F. Ruiz, M. Parraga, M. J. Garcia-Ortiz, T. Kirchhoff, J. del Mazo, A. Bernad, and L. Blanco. 2000. DNA polymerase lambda (Pol  $\lambda$ ), a novel eukaryotic DNA polymerase with a potential role in meiosis. *J. Mol. Biol.* **301**:851–867.
11. Grawunder, U., D. Zimmer, S. Fugmann, K. Schwarz, and M. R. Lieber. 1998. DNA ligase IV is essential for V(D)J recombination and DNA double-strand break repair in human precursor lymphocytes. *Mol. Cell* **2**:477–484.
12. Insel, R. A., and W. S. Varade. 1998. Characteristics of somatic hypermutation of human immunoglobulin genes. *Curr. Top. Microbiol. Immunol.* **229**:33–44.
13. Ito, J., and D. K. Braithwaite. 1991. Compilation and alignment of DNA polymerase sequences. *Nucleic Acids Res.* **19**:4045–4057.
14. Johnson, R. E., M. T. Washington, L. Haracska, S. Prakash, and L. Prakash. 2000. Eukaryotic polymerases  $\iota$  and  $\zeta$  act sequentially to bypass DNA lesions. *Nature* **406**:1015–1019.
15. Johnson, R. E., M. T. Washington, S. Prakash, and L. Prakash. 2000. Fidelity of human DNA polymerase  $\eta$ . *J. Biol. Chem.* **275**:7447–7450.
16. Kornberg, A., and T. Baker. 1991. DNA replication, 2nd ed. W. H. Freeman, New York, N.Y.
17. Kubota, Y., R. A. Nash, A. Klungland, P. Schar, D. E. Barnes, and T. Lindahl. 1996. Reconstitution of DNA base excision-repair with purified human proteins: interaction between DNA polymerase beta and the XRCC1 protein. *EMBO J.* **15**:6662–6670.
18. Levy, Y., N. Gupta, F. Le Deist, C. Garcia, A. Fischer, J. C. Weill, and C. A. Reynaud. 1998. Defect in IgV gene somatic hypermutation in common variable immunodeficiency syndrome. *Proc. Natl. Acad. Sci. USA* **95**:13135–13140.
19. Matsuda, T., K. Bebenek, C. Masutani, F. Hanaoka, and T. A. Kunkel. 2000. Low fidelity DNA synthesis by human DNA polymerase  $\eta$ . *Nature* **404**:1011–1013.
20. McDonald, J. P., V. Raptic-Otrin, J. A. Epstein, B. C. Broughton, X. Wang, A. R. Lehmann, D. J. Wolgemuth, and R. Woodgate. 1999. Novel human and mouse homologs of *Saccharomyces cerevisiae* DNA polymerase  $\eta$ . *Genomics* **60**:20–30.
21. Morrison, A., R. B. Christensen, J. Alley, A. K. Beck, E. G. Bernstine, J. F. Lemontt, and C. W. Lawrence. 1989. REV3, a *Saccharomyces cerevisiae* gene whose function is required for induced mutagenesis, is predicted to encode a nonessential DNA polymerase. *J. Bacteriol.* **171**:5659–5667.
22. Nelson, J. R., C. W. Lawrence, and D. C. Hinkle. 1996. Thymine-thymine dimer bypass by yeast DNA polymerase  $\zeta$ . *Science* **272**:1646–1649.
23. Ohashi, E., K. Bebenek, T. Matsuda, W. J. Feaver, V. L. Gerlach, E. C. Friedberg, H. Ohmori, and T. A. Kunkel. 2000. Fidelity and processivity of DNA synthesis by DNA polymerase  $\kappa$ , the product of the human *DINB1* gene. *J. Biol. Chem.* **275**:39678–39684.
24. Ohmori, H., E. C. Friedberg, R. P. P. Fuchs, M. F. Goodman, F. Hanaoka, D. Hinkle, T. A. Kunkel, C. W. Lawrence, Z. Livneh, T. Nohmi, L. Prakash, S. Prakash, T. Todo, G. C. Walker, Z. Wang, and R. Woodgate. 2001. The Y-family of DNA polymerases. *Mol. Cell* **8**:7–8.
25. Rathmell, W. K., and G. Chu. 1998. Mechanisms for DNA double-strand break repair in eukaryotes, p. 299–316. *In* J. A. Nickoloff, and M. F. Hoekstra (ed.), DNA damage and repair, vol. II. Humana Press, Totowa, N.J.
26. Ruiz, J. F., O. Dominguez, T. Lain de Lera, M. Garcia-Diaz, A. Bernad, and L. Blanco. 2001. DNA polymerase mu, a candidate hypermutase? *Phil. Trans. R. Soc. Lond. B* **356**:99–109.
27. Sharief, F. S., P. J. Vojta, P. A. Ropp, and W. C. Copeland. 1999. Cloning and chromosomal mapping of the human DNA polymerase theta (POL $\theta$ ), the eighth human DNA polymerase. *Genomics* **59**:90–96.
28. Tissier, A., J. P. McDonald, E. G. Frank, and R. Woodgate. 2000. pol $\iota$ , a remarkably error-prone human DNA polymerase. *Genes Dev.* **14**:1642–1650.
29. Waga, S., and B. Stillman. 1998. The DNA replication fork in eukaryotic cells. *Annu. Rev. Biochem.* **67**:721–751.
30. Wagner, S. D., and M. S. Neuberger. 1996. Somatic hypermutation of immunoglobulin genes. *Annu. Rev. Immunol.* **14**:441–457.
31. Wang, Z. 2001. Translesion synthesis by the UmuC family of DNA polymerases. *Mutat. Res.* **486**:59–70.
32. Weaver, D. T. 1995. V(D)J recombination and double-strand break repair. *Adv. Immunol.* **58**:29–85.
33. Wilson, S. H. 1998. Mammalian base excision repair and DNA polymerase  $\beta$ . *Mutat. Res.* **407**:203–215.
34. Wilson, T. E., U. Grawunder, and M. R. Lieber. 1997. Yeast DNA ligase IV mediates non-homologous DNA end joining. *Nature* **388**:495–498.
35. Wilson, T. E., and M. R. Lieber. 1999. Efficient processing of DNA ends during yeast nonhomologous end joining. Evidence for a DNA polymerase  $\beta$  (Pol4)-dependent pathway. *J. Biol. Chem.* **274**:23599–23609.
36. Wood, R. D., and M. K. Shivji. 1997. Which DNA polymerases are used for DNA-repair in eukaryotes? *Carcinogenesis* **18**:605–610.
37. Xin, H., W. Lin, W. Sumanasekera, Y. Zhang, X. Wu, and Z. Wang. 2000. The human *RAD18* gene product interacts with HHR6A and HHR6B. *Nucleic Acids Res.* **28**:2847–2854.
38. Zhang, Y., F. Yuan, X. Wu, and Z. Wang. 2000. Preferential incorporation of G opposite template T by the low-fidelity human DNA polymerase  $\iota$ . *Mol. Cell. Biol.* **20**:7099–7108.
39. Zhang, Y., F. Yuan, H. Xin, X. Wu, D. Rajpal, D. Yang, and Z. Wang. 2000. Human DNA polymerase  $\kappa$  synthesizes DNA with extraordinarily low fidelity. *Nucleic Acids Res.* **28**:4147–4156.